

# Implementation of electrochemical, optical and denuder-based sensors and sampling techniques on UAV for volcanic gas measurements: examples from Masaya, Turrialba and Stromboli Volcanoes

5 Julian Rüdiger<sup>1,\*</sup>, Lukas Tirpitz<sup>2</sup>, J. Maarten de Moor<sup>3</sup>, Nicole Bobrowski<sup>2,4,5</sup>, Alexandra Gutmann<sup>1</sup>,  
Marco Liuzzo<sup>6</sup>, Martha Ibarra<sup>7</sup> and Thorsten Hoffmann<sup>1</sup>

<sup>1</sup>Johannes Gutenberg-University, Institute of Inorganic and Analytical Chemistry, Mainz, Germany

<sup>2</sup>Institute for Environmental Physics, Heidelberg

<sup>3</sup>Observatorio Vulcanológico y Sismológico de Costa Rica, Heredia, Costa Rica

10 <sup>4</sup>Johannes Gutenberg-University, Institute of Geosciences, Mainz, Germany

<sup>5</sup>Max Planck Institute for Chemistry, Mainz, Germany

<sup>6</sup>Istituto Nazionale di Geofisica e Vulcanologia, Sezione di Palermo, Italy

<sup>7</sup>Instituto Nicaragüense de Estudios Territoriales, Managua, Nicaragua

15 \* now at University of Bayreuth, Atmospheric Chemistry, Bayreuth, Germany.

*Correspondence to:* Julian Rüdiger (j.ruediger@uni-mainz.de) and Thorsten Hoffmann (hoffmant@uni-mainz.de)

**Abstract.** Volcanoes are a natural source of several reactive gases (e.g. sulfur and halogen containing species), as well as non-reactive gases (e.g. carbon dioxide) to the atmosphere. The relative abundance of carbon and sulfur in volcanic gas as well as the total sulfur dioxide emission rate from a volcanic vent are established parameters in current volcano monitoring strategies, 20 and they oftentimes allow insights into subsurface processes. On the other hand, chemical reactions involving halogens are thought to have local to regional impact on the atmospheric chemistry around passively degassing volcanoes. In this study we demonstrate the successful deployment of a multirotor UAV (quadcopter) system with custom-made lightweight payloads for the compositional analysis and gas flux estimation of volcanic plumes. The various applications and their potential are presented and discussed on example studies at three volcanoes encompassing flight heights of 450 m to 3300 m and various 25 states of volcanic activity. Field applications were performed at Stromboli Volcano (Italy), Turrialba Volcano (Costa Rica) and Masaya Volcano (Nicaragua). Two in-situ gas-measuring systems adapted for autonomous airborne measurements, based on electrochemical and optical detection principles, as well as an airborne sampling unit, are introduced. We show volcanic gas composition results including abundances of CO<sub>2</sub>, SO<sub>2</sub> and halogen species. The new instrumental set-ups were compared with established instruments during ground-based measurements at Masaya volcano, which resulted in CO<sub>2</sub>/SO<sub>2</sub> ratios of 3.6 30 ± 0.4. For total SO<sub>2</sub> flux estimations a small differential optical absorption spectroscopy (DOAS) system measured SO<sub>2</sub> column amounts on transversal flights below the plume at Turrialba Volcano, giving 1776 ± 1108 T/d and 1616 ± 1007 T/d of SO<sub>2</sub> during two traverses. At Stromboli volcano, elevated CO<sub>2</sub>/SO<sub>2</sub> ratios have been observed in spatial and temporal proximity to

explosions by airborne in-situ measurements. Reactive bromine to sulfur ratios of  $0.19 \times 10^{-4}$  to  $9.8 \times 10^{-4}$  were measured in-situ in the plume of Stromboli volcano downwind of the vent.

## 1 Introduction

Gaseous volcanic emissions consist of a variety of different compounds and are dominated by water vapor ( $\text{H}_2\text{O}$ ), carbon dioxide ( $\text{CO}_2$ ), sulfur dioxide ( $\text{SO}_2$ ), and hydrogen sulfide ( $\text{H}_2\text{S}$ ) (Symonds et al., 1994). Minor abundant, but nonetheless important gas species are halogen-bearing compounds which are emitted as hydrogen halides ( $\text{HF}$ ,  $\text{HCl}$ ,  $\text{HBr}$  and  $\text{HI}$ ) and later partly transformed by heterogeneous reactions into other halogen species, such as bromine monoxide ( $\text{BrO}$ ) or chlorine dioxide ( $\text{OCIO}$ ) (Bobrowski et al., 2007). The relative gas composition varies with the types of volcanoes and magmas as well as with transport and degassing mechanisms. Changes in the magma degassing behavior and/or the hydrothermal systems beneath 10 volcanoes generally influence the gas composition and gas fluxes. Measuring the emitted gas composition can provide crucial information on understanding subsurface processes related to activity changes (e.g. Allard et al., 1991; Aiuppa et al., 2007; Bobrowski and Giuffrida, 2012; de Moor et al., 2016a; Liotta et al., 2017) and help to estimate fluxes of the geological carbon cycle (e.g. Burton et al., 2013; Mason et al., 2017) and tectonic processes controlling volcanic degassing (e.g. Aiuppa et al., 2017; de Moor et al. 2017). In the field of volcanic monitoring, the observation of gas composition changes has become an 15 important tool for detecting precursory processes for volcanic eruptions. For instance, the  $\text{CO}_2/\text{SO}_2$  emission ratio strongly varies with volcanic activity, which is associated to magma rising up a conduit. The solubility of magmatic gases is pressure dependent and different gases are released from the magma at different depths during the magma ascent, that is accompanied by pressure decrease. Gas ratio changes have been observed within the timescale of hours to weeks prior to eruptions (e.g. Giggenbach, 1975; Aiuppa et al., 2007; de Moor et al., 2016a, de Moor et al., 2016b) and their magnitude, direction, and pace 20 are highly variable throughout different volcanic systems and state of activity. In-situ measurements of this gas ratio has become a well-established method using electrochemical ( $\text{SO}_2$ ) and infrared ( $\text{CO}_2$ ) sensors, implemented in so-called Multi-GAS (MG) instruments, which may also contain other sensors and are field-deployable to work autonomously close to volcanic emission sources (Shinohara, 2005; Aiuppa et al., 2006). Another important parameter for the characterization of volcanic activity is the gas emission rate. Particularly, the determination of  $\text{SO}_2$  flux has become a standard procedure by traversing the 25 plume and multiplying the integrated  $\text{SO}_2$  cross-section with the estimated plume transport speed (e.g. McGonigle et al., 2002; Galle et al., 2003; López et al., 2013). With the development of small DOAS instruments, traversing the plume is not only feasible by cars, boats, or manned aircraft, but also by walking in case of poorly accessible terrain. Furthermore, knowledge about in-plume chemical reactions can be drawn from compositional assessment of the gases, which also helps understanding their impact on atmospheric chemistry (e.g. Lee et al., 2005; Glasow et al., 2009, von Glasow, 2010; Gliß et al., 2015). 30 Especially the halogen chemistry is of great interest as  $\text{BrO}/\text{SO}_2$  ratios in volcanic plumes are readily measurable by remote sensing UV spectrometry (e.g. Bobrowski et al., 2003, Lübcke et al., 2014) and have been discussed in recent years as another potential precursory observable for volcanic activity changes. Although several studies observed decreases in the  $\text{BrO}/\text{SO}_2$

ratio in advance to eruptive phases (e.g. Lübecke et al., 2014) and lower ratios during periods of continuous activity (Bobrowski and Giuffrida, 2012), it is not yet clear whether magma-gas partitioning of bromine occurs prior or after sulfur during the pressure drop associated with magma ascents (Dinger et al., 2017). Furthermore, BrO is not a directly emitted species rather than the product of complex heterogeneous chemistry in the volcanic plume involving reactions with magmatic gases with 5 entrained air (e.g. Gerlach, 2004, Bobrowski et al., 2007). The variation of BrO by plume age and a transversal distribution in the plume for this species was observed by differential optical absorption spectroscopy (DOAS) measurements (Bobrowski et al., 2007). Additionally, other reactive halogen species with oxidation states  $\neq -1$  (e.g. Br<sub>2</sub>, Cl<sub>2</sub>, BrCl and others) have been measured in-situ in the plume of Mt. Etna, Italy (Rüdiger et al., 2017) and Mt Nyamuragira (Bobrowski et al., 2017). In the last decade, several model studies (e.g. Bobrowski et al., 2007, Roberts et al., 2009; von Glasow, 2010; Roberts et al., 2014; 10 Jourdain et al., 2016) have engaged on the variation of halogen variability in volcanic plumes with respect to various atmospheric and magmatic parameters. In the case of bromine, it was modelled that the initial emitted hydrogen bromide is depleted shortly after emission under consumption of tropospheric ozone and is transformed to reactive species such as BrO, HOBr, Br<sub>2</sub>, BrCl and BrONO<sub>2</sub>. Due to the challenging task of accessing volcanic plumes on a timescale of minutes after emission, and the lack of spectroscopic methods for most of these reactive species, uncertainties about their relative abundances 15 still exist. One approach towards the in-situ observation of reactive halogen species is the application of gas diffusion denuder sampling using a selectively reactive organic coating (1,3,5-trimethoxybenzen, TMB) to trap and enrich gaseous species containing a halogen atom with the oxidations state +1 or 0 (e.g. Br<sub>2</sub> or BrCl), while being insensitive to the particle phase (Rüdiger et al., 2017).

In the case of most volcanoes sampling on the crater rim may be associated with considerable logistical challenges and hazards 20 for people and instruments. During phases of high activity crater rims are usually not accessible at all and even during quiescent degassing work at the crater rim represents a considerable risk. However, the knowledge of plume gas composition is an important component for activity assessments of volcanoes (e.g. Carroll and Holloway, 1994; Aiuppa et al., 2006) and therefore gas monitoring stations are deployed and maintained in close proximity to active volcanic vents by researchers, putting themselves at risks. Advancements in the application of remote sensing techniques have helped to minimize personnel 25 exposition to the volcanic danger zone (e.g. Galle et al., 2003; Tamburello et al., 2011). However, still today the detection of certain gas species and/or total amounts of all species of an element is not possible remotely (neither ground based nor with satellites) and therefore in-situ measurements are an important tool, especially for resolving chemical reactions and speciation changes in aging volcanic plumes. With an in-situ sampling strategy, obtaining samples from the freshly emitted plume is feasible, while ground-based in-situ sampling of the aged plume further downwind is rarely possible and dependent on specific 30 wind and geographical conditions. As in the last decade with the development of compact and cost effective unmanned aerial vehicles (UAV) several deployments of gas sensors and other in-situ methods (e.g. particle detection (Altstädter et al., 2015)) as well as applications of spectrometers were realized (e.g. McGonigle et al., 2008, Diaz et al., 2015, Mori et al., 2016, Villa et al., 2016 and references therein)., Pioneering UAV deployments were already conducted in the late 70's (Faivre-Pierret et al., 1980). While these drone-based applications focused mostly on the use of sensors and spectroscopy methods, we present

here a low-cost UAV-deployable sampling (gas diffusion denuder) and sensing (electrochemical/optical sensors) systems for the determination of CO<sub>2</sub>, SO<sub>2</sub> and halogen species. Our system enabled us to access the plume close to an active vent as well as the aged plume several km downwind of the source and elevated from ground, without exposing operators to the risks in proximity to active vents or employing manned aircrafts to potential engine-damaging ash and gas plumes. In addition to that, 5 the UAV-deployment of a lightweight DOAS instrument for SO<sub>2</sub> flux estimations is presented herein, which enables fast plume traversing in terrains that are usually not accessible by cars or even by foot.

## 2. Site description

### 2.1 Stromboli

Stromboli volcano, the northernmost island of the Aeolian volcanic arc (Italy), rises 924 m above sea level (a.s.l.). The island 10 represents the top part of a large 2500-m-high stratovolcano emerging from the Tyrrhenian Sea floor. Stromboli is well known for its regular (~ every 10-20 min) explosive activity (Strombolian activity). Intermittently, continuous passive degassing occurs from the active vents, which are located in the so-called crater terrace at about 750 m a.s.l.. Ejected lava material is dominantly deposited in a northwestern direction, forming a horseshoe-shaped area (Sciara del Fuoco) that is not safely 15 accessible on foot. The summit above the craters is well accessible, and numerous monitoring stations have been installed here for continuous observation of the ongoing volcanic activity. Thus, Stromboli has been a laboratory volcano for studying magma degassing processes (Allard et al. 2008) and field-testing new instrumentations for many years.

While most gas monitoring station positions benefit from a north westerly wind direction, a south easterly wind only allows 20 gas plume detection by spectroscopic methods. In this study, due to the dominance of southeast winds in early April 2016 an approach from an eastern direction was chosen, using a multicopter as carrier for gas sampling and sensing instruments. The UAV was mostly launched at the northern shelter (see Fig. 1).

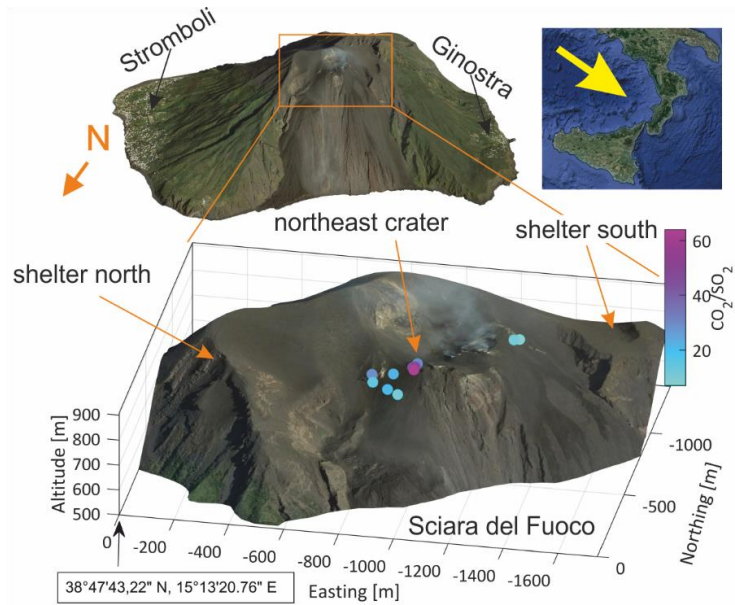


**Figure 1: Overview of the sampling site at Stromboli Volcano with the locations of the retrieved CO<sub>2</sub>/SO<sub>2</sub> mixing ratios given in Table 2**

## 2. 2 Masaya

5 Masaya volcano (elevation ~ 600 m a.s.l.), Nicaragua, is a basaltic-andesite shield volcano caldera (6 x 11 km in size) hosting a set of vents. The currently active vent is situated in the Santiago pit crater, formed in 1858-1859 (McBirney, 1956). Masaya persistently emits voluminous quantities of SO<sub>2</sub>, with fluxes typically ranging from 500 T/d to 2500 T/d (e.g. (Mather et al., 2006; de Moor et al., 2013; Carn et al., 2017), making this volcano currently to one of the largest contributor to volcanic gas emissions in the Central American Volcanic Arc (de Moor et al. 2017). In January 2016 the reoccurrence of a new superficial  
10 lava lake (~40 x 40 m) was observed together with an increase in activity. Due to high emission rates and the low-altitude plume, Masaya volcano has a detrimental environmental impact on the downwind areas, diminishing vegetation and potentially affecting human health (Delmelle et al., 2002). Continuous monitoring of the gas emissions is realized by a stationary Multi-GAS (MG) system (through the Deep Carbon Observatory – Deep Earth Carbon Degassing initiative (DCO-DECADE)) at the crater rim and two scanning DOAS instruments (Network for Observation of Volcanic and Atmospheric Change (NOVAC)  
15 (Galle et al., 2010)) in the downwind direction. Besides the presence of a strong plume, Masaya volcano provides perfect conditions for field-testing new methods and studying plume chemistry using UAVs: easy accessibility by car, low altitude, and relative stable dominant wind direction (northeast). In July 2016 flights were launched from the caldera bottom marked “flight area” in Fig. 2 (c).

## 2. 3 Turrialba

Turrialba is a stratovolcano with a peak elevation of 3340 m a.s.l. and is located about 35 km east and directly upwind of San José, the capital of Costa Rica. It is the southernmost active volcano of the Central American Volcanic Arc. In the 2000s, an almost 150 years long period of quiescence has ended and since 2010 several vent opening phreatic eruptions henceforth occurred marking an ongoing but erratic phase of unrest (Martini et al., 2010), characterized by variable ash and gas emission intensities (up to 5000 tons/day of SO<sub>2</sub> (de Moor et al., 2016a)), making Turrialba volcano to the second substantial emitter in the arc, besides Masaya volcano (de Moor et al. 2017). The proximity of Turrialba volcano to the densely populated central valley with Costa Rica's major international airport and the dominant western wind direction is responsible for ash depositions, causing health and air traffic problems. Therefore, the activity of Turrialba is continuously monitored by various systems including permanent Multi-GAS stations to observe short-term precursory changes in the gas composition prior to eruptive events (de Moor et al., 2016a). However, stations located near the active vent suffer from ash deposition and ballistic impacts during more frequent episodes, making maintenance demanding and risky or impossible. Furthermore, the accessibility of the summit and surrounding areas is degrading due to intense erosion following vegetation destruction by acid rain, heavy rainfall, ash deposition and remobilization, and the lack of infrastructural maintenance following community evacuation. Thus, the use of UAV-based systems might represent the only viable approach for in-situ measurements of the open vent plume during periods of high activity. In 2016 flights were conducted starting at the "La Silva" site (Fig. 2 (d)) to investigate the feasibility of UAV-based gas sensing system at this challenging environment (high altitude and thick ash plumes).

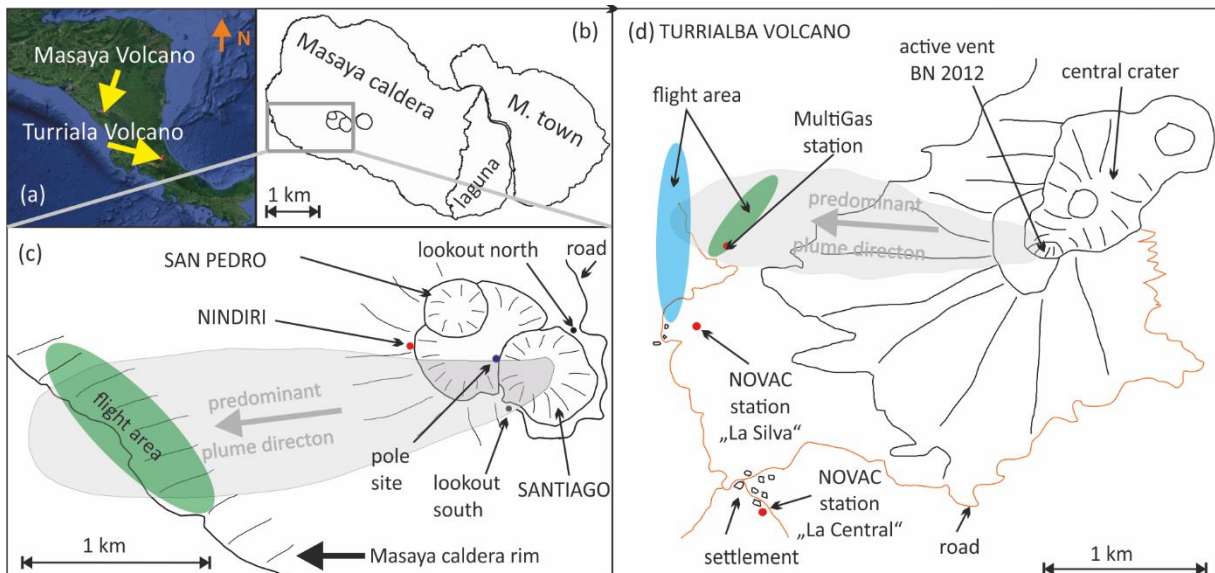


Figure 2: Overview on the field work sites at (a-c) Masaya volcano (Nicaragua) and (d) Turrialba volcano (Costa Rica). Sampling locations mentioned in Table 3 are marked in (c) as follows: Santiago rim, lookout south (black marker); Santiago rim, pole site (blue marker); Nindiri rim (red marker)

### 3. Instrumentation

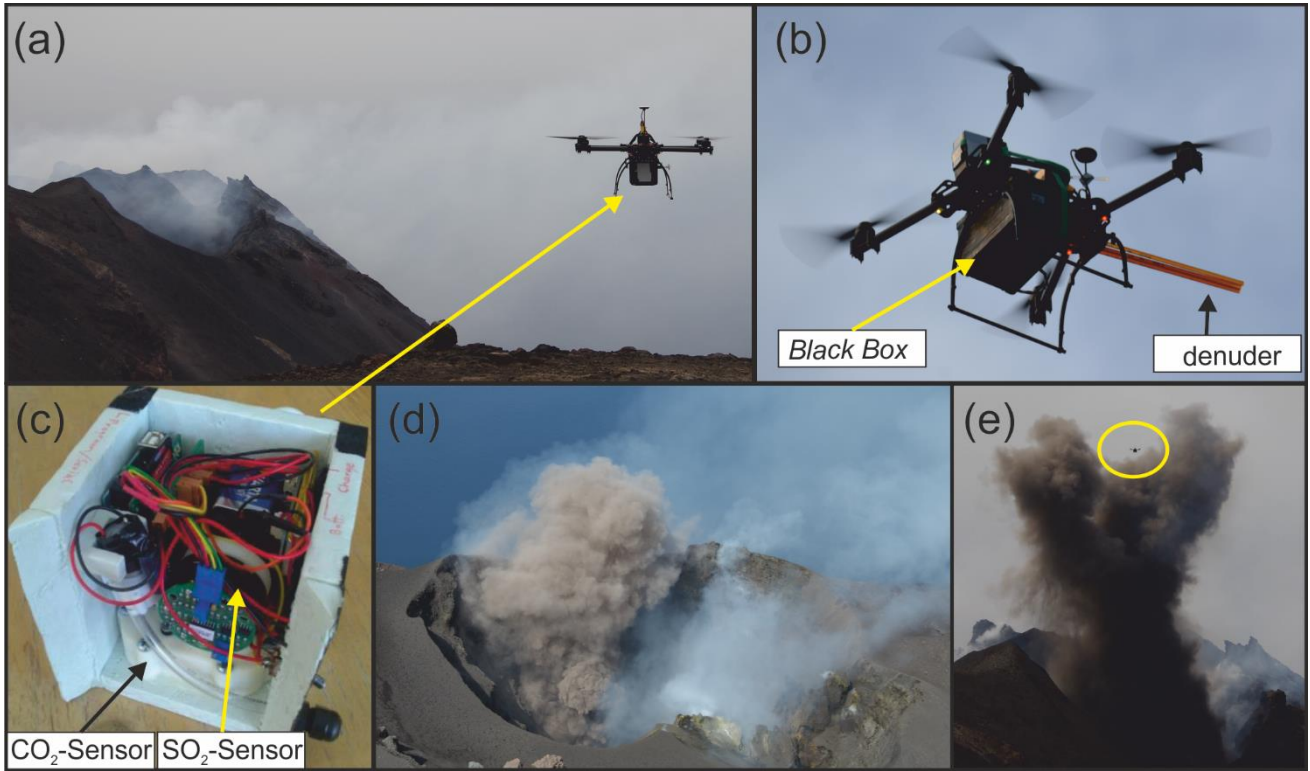
#### 3.1 Unmanned aerial vehicle

The UAV (called RAVEN, ~~remote-controlled aircraft for volcanic emission analysis~~, see Fig. 3 (a) – (b)) used during the field campaigns was a four-rotor multicopter with foldable arms (Black Snapper, Globe Flight, Germany) with an E800 motor set

5 using propellers with a diameter of 13 inch and a pitch of 4.5 inch (DJI Innovations, Shenzhen, China). It was flown manually in line-of-sight conditions. The multicopter had a weight of 2.3 kg including a 22.2 V (6S) 4.5 Ah battery. A maximum payload of 1.3 kg was achieved with various mounted instruments. The foldable frame of the UAV was beneficial in regards of the usual necessity to personally carry equipment into field, especially on volcanoes like Stromboli. Another advantage of this system was that the battery capacity is within the guidelines of air travel restrictions allowing the system to be transported on

10 commercial airplanes. The main controller (NAZA M-2, DJI Innovations, Shenzhen, China) of the multicopter was connected with a combined denuder sampling and SO<sub>2</sub> sensing instrument (hereafter named Black Box (see Sec. 3.3)), to transmit the measured SO<sub>2</sub> data as an 0 V - 5 V signal to the remote control, where it is displayed. This allowed the operator to find areas with dense plume in which to hover the system for stationary sampling and to react to changes of the plume direction, which is challenging if relying only on visual observation of the plume. A data logger (Core 2, Flytrex Aviation, Tel Aviv, Israel)

15 with micro SD card was used to log the flight data from the main controller consisting of GPS coordinates, pressure and temperature data at 2 Hz. The payloads were attached below the main body of the multicopter with an inlet for the in-situ CO<sub>2</sub> and SO<sub>2</sub> sensing instrument (hereafter called Sunkist (see Sec. 3.2)) close to the center of the copter. The sampled air volume can be assumed to originate from within a radius of a few meters around the inlet (see e.g. Roldan et al., 2015; Alvarado et al., 2017; Palomaki et al., 2017), which represents homogeneous plume gas for a widely spread out plume. This assumption is 20 confirmed by a self-developed method for the estimation of the origin of sample air, which is described in the supplementary material (Chapter IV).



5 **Figure 3:** (a) Sampling site at Stromboli Volcano with Northeast crater in the background and the *RAVEN* UAV carrying the *Sunkist* gas monitor, (b) *RAVEN* UAV with the Black Box sampling unit and three gas diffusion denuders, (c) interior view of the *Sunkist* gas monitor, showing the CO<sub>2</sub> and SO<sub>2</sub> sensors, (d) passive degassing (white plume) and eruptive ash explosion (brown ash cloud) at the north east crater at Stromboli Volcano, (e) ash eruption at the Northeast crater producing an ascending ash plume with the *RAVEN* UAV in direct proximity (yellow circle), returning from sampling flight

### 3.2 CO<sub>2</sub>/SO<sub>2</sub> gas sensors – Multi-GAS (Sunkist)

A gas sensor system was developed for use in volcanic environments with a focus on robustness and compact and lightweight design for application on UAVs. The system, called Sunkist (SK) contains two gas sensors: (1) A CO<sub>2</sub> sensor (K30 FR, 10 SenseAir, Delsbo, Sweden), which uses the principle of non-dispersive infra-red absorption spectroscopy: The sample gas gets sucked into a multi reflection cell, where it is exposed to the radiation of a small infra-red light source. The CO<sub>2</sub> concentration is determined by measuring the light attenuation on distinct CO<sub>2</sub> absorption bands in the near infra-red. (2) An electrochemical SO<sub>2</sub> sensor (CiTiceL 3MST/F, City Technology, Portsmouth, United Kingdom), which basically consists of an electrochemical cell, where oxidation of SO<sub>2</sub> on one of the cell's electrodes creates charges and leads to a measureable compensating current 15 between the two cell electrodes.

**Table 1: Components and specifications of the sampling and sensing instruments**

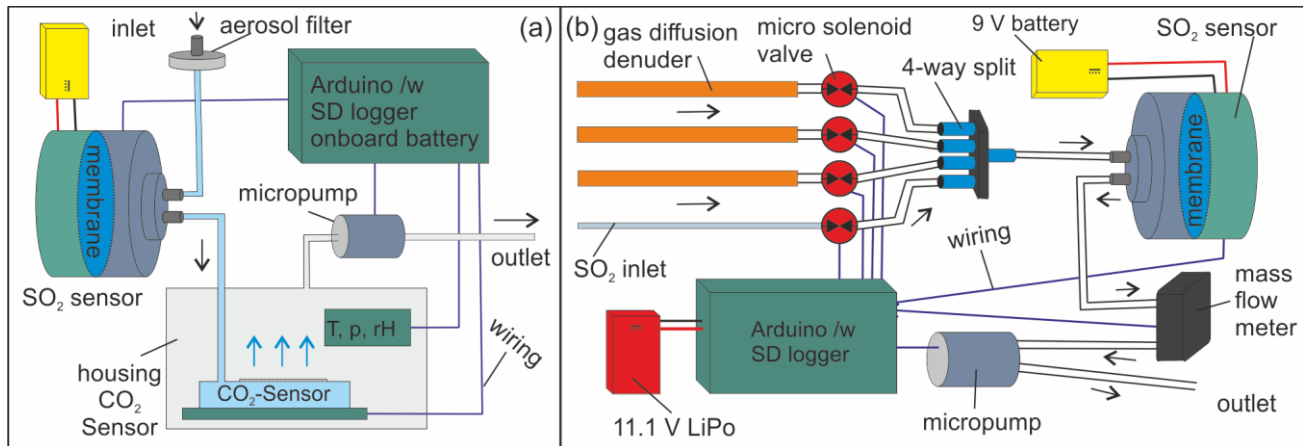
| Component/ | Specifications |           |
|------------|----------------|-----------|
| Parameter  | Sunkist        | Black Box |

|                               |  |  |  |
|-------------------------------|--|--|--|
| <b>CO<sub>2</sub> sensor</b>  | NDIR, SenseAir CO <sub>2</sub> Engine K30 FR   |  |  |
| <b>SO<sub>2</sub> sensor</b>  | Electrochemical, CiTiceL 3MST/F  |  | Electrochemical, CiTiceL 3MST/F  |
| <b>Operating temperature</b>  | 0-50°C (CO <sub>2</sub> ), -20-50°C (SO <sub>2</sub> )                               |  | -20-50°C   |
| <b>Operating humidity</b>     | 0-95% (CO <sub>2</sub> ), 15-90% (SO <sub>2</sub> ), non-condensing                  |  | 15-90% (SO <sub>2</sub> ), non-condensing  |
| <b>Operating pressure</b>     | Atmospheric ± 10% (SO <sub>2</sub> )   |  | Atmospheric ± 10%  |
| <b>Temperature dependence</b> | 1/T (assumed for CO <sub>2</sub> ), 0.25 %/°C (SO <sub>2</sub> )                     |  | 0.25 %/°C  |
| <b>Pressure dependence</b>    | 1.6 %/kPa (CO <sub>2</sub> ), 0.0015 %/kPa (SO <sub>2</sub> ) <sup>#</sup>           |  | 0.0015 %/kPa <sup>#</sup>  |
| <b>Response time</b>          | 2 s (CO <sub>2</sub> ), <20 s (SO <sub>2</sub> )                                     |  | <20 s  |
| <b>Accuracy</b>               | ± 30 ppm ± 5 % signal (CO <sub>2</sub> ),<br>± 1 ppm ± 1 % signal (SO <sub>2</sub> ) |  | ± 1ppm ± 1 % signal  |
| <b>Instrument noise (1σ)</b>  | 5 ppm (CO <sub>2</sub> ), 0.05 ppm (SO <sub>2</sub> )                                |  | 0.05 ppm   |
| <b>Range</b>                  | 0-5000 ppm (CO <sub>2</sub> ), 0-200 ppm (SO <sub>2</sub> )                          |  | 0-100 ppm  |
| <b>Sampling rate</b>          | 2 Hz   |  | 2 Hz   |
| <b>Computer</b>               | Arduino, with microSD card logger  |  | Arduino, with SD card data logger and motor-shield to power the pump                           |
| <b>Voltage</b>                | 9 V for SO <sub>2</sub> sensor (alkaline battery),<br>3.7 V LiPo battery for Arduino |  | 9 V for SO <sub>2</sub> sensor (alkaline battery),<br>11.1 V LiPo battery for Arduino and pump |
| <b>Inlet</b>                  | particle filter  |  | 3 denuders (50 cm) or 3 x 2 denuders (15 cm)   |
| <b>Others</b>                 | Warm up time   | 1 min (CO <sub>2</sub> )                 | Micro solenoid valves<br>First Sensor, Germany<br>TN2P006LM05LB                                |
|                               | Additional Sensors   | Temperature, pressure, relative humidity | Mass flow meter<br>First Sensor, Germany, WBAL001DUH0  |
|                               |  |  | Micro pump<br>TCS micropumps, UK, DS250BL  |
| <b>Weight</b>                 | 500 g  |  | 500 g  |
| <b>Dimensions</b>             | 14x13x14 cm (LxWxH)  |  | 20x13x14 cm (LxWxH)  |

# The pressure dependence of 0.0015 %/kPa is a second order effect and is negligible for our application

The CO<sub>2</sub> sensor is placed inside a hermetic box, which is part of the air path (Fig. 4 (a)). It is equipped with further on-chip sensors for humidity (SHT21 from Sensirion, Staefa, Switzerland), temperature and pressure (BMP180 by Bosch Sensortec, Reutlingen, Germany), which allow to correct the gas data for dependencies on named environmental parameters.

The sensors are read out by a custom-built Arduino Uno Rev 3 computer with a micro SD card logger at a sampling rate of 2 Hz and powered by a rechargeable 3.7 V lithium polymer (LiPo) battery (Fig. 4 (b)). The SO<sub>2</sub> sensor was powered by a separate 9 V alkaline battery. The whole system is sheltered in a polystyrene foam case and has a total weight of 500 g (Fig. 3 (c)). A 45- $\mu$ m pore size PTFE filter was attached to the inlet to prevent particles from entering the sensors. Gas was pumped through to the sensors in series (1. SO<sub>2</sub>, 2. CO<sub>2</sub>) by a small pump using a flow rate of 500 ml/min. The system was calibrated before and after field deployments with CO<sub>2</sub> (0-1500 ppm) and SO<sub>2</sub> (0-30 ppm) test gases. Detailed information on the specifications of the sensors is shown in Table 1 and in the supplementary material (Fig. S1).



10 **Figure 4: Schematics of the (a) Sunkist monitoring unit and the (b) Black Box gas sampling system**

### 3.3 Gas diffusion denuder sampler (Black Box)

An in-situ gas sampling system was constructed to enable gas diffusion denuder sampling in the plume at various distances from the vent using the UAV. To compensate for dilution, a CiTiceL 3MST/F SO<sub>2</sub> sensor (City Technology, Portsmouth, United Kingdom) was implemented to obtain halogen/sulfur ratios combining denuder samples and sensor data. The sampler (called Black Box (BB)) consisted of the following components, which are introduced in the order the gas passes through: I) inlet system for three denuders; II) electrochemical SO<sub>2</sub> sensor; III) mass flow sensor; IV) micro gas pump (see Figure 4 (b) and Table 1). The housing was made of polystyrene foam to ensure that weight requirements were met. An Arduino microcontroller (Uno Rev 3) for signal processing and data logging on a SD card was built in. Various 11.1 V LiPo batteries (500 and 1000 mAh) supplied the power, with different capacities depending on the desired payload and operation time. The Arduino computer transmitted a pulse width modulated signal between 0 V and 5 V, proportional to the detected SO<sub>2</sub> mixing ratio, to the main controller of the multicopter via cable connection, which then was sent by telemetry to the remote control to allow the operator to assess plume strength in real time to optimize denuder exposure time. The SO<sub>2</sub> gas sensor was calibrated in the laboratory and close to field conditions with SO<sub>2</sub> gas standards in N<sub>2</sub> (0 – 54.1 ppm).

Gas diffusion denuder sampling, which enriches gaseous compounds while being insensitive to the particle phase, was applied by using two types of coating materials as derivatization agent for the gas diffusion sampling. Total gaseous reactive molecular bromine species, BrX (Br<sub>2</sub>, BrCl, (H)OBr), were determined by denuders coated with 15 µmol of 1,3,5-trimethoxybenzene (TMB) - which reacts to 1-bromo-2,4,6-trimethoxybenzene - and subsequent gas chromatography-mass spectrometry (GC-MS) analysis (Rüdiger et al., 2017). Hydrogen bromide (HBr) was sampled with denuders coated with 7.2 µmol of 5,6-epoxy-5,6-dihydro-1,10-phenanthroline (EP) - which is selectively reactive towards halogen acids through its epoxy function forming 5-halogeno-6-hydroxy-5,6-dihydro-1,10-phenanthroline - and analyzed by liquid chromatography-mass spectrometry (LC-MS). For the UAV-based application 15 cm long denuders were used at a sampling flow rate of 208 ml/min to ensure quantitative sampling. Denuders with both coating types were sampled at the same flow rate simultaneously to the recording of Multi-GAS (Sunkist) data.

### **3.4 Drone-operated miniature differential optical absorption spectroscopy (DROAS)**

A miniature UV spectrometer system (Galle et al., 2003) was employed for flying mobile DOAS traverse measurements to conduct estimations of the SO<sub>2</sub> flux at Turrialba volcano. This system consisted (Fig. 8 (a)) of an UV spectrometer (USB2000+, Ocean Optics, USA), a miniature telescope (Ocean Optics 74-DA collimating lens, diameter: 5 mm, focal length 10 mm), a GPS Antenna (BU-353-S4, GlobalSat, Taipei, Taiwan) and a miniature on-board computer (VivoStick TS10, ASUS, Taipei, Taiwan). The system was powered by a 11.1 V LiPo battery (1000 mAh), which was connected via a switching regulator (CC BEC 10 A, Castle Creations, USA) to give 9 V at 2 A. The spectrometer and the GPS antenna were connected (and powered) at the computer via USB ports. The NOVAC software “mobile DOAS” developed at the Chalmers University (Sweden) was run on the computer for data acquisition and later evaluation. The miniature PC in the spectrometer system was accessed via a remote desktop connection by a different computer to initialize the data acquisition by the “mobile DOAS” software. Validation of the SO<sub>2</sub> fluxes obtained by DROAS traverses was achieved by a comparison with the SO<sub>2</sub> fluxes derived by two NOVAC stationary DOAS instruments (*La Silva* and *La Central*, see Fig. 2 (d)) located in proximity to the flight area.

### **3.5. Data Processing**

#### **3.5.1 Sensor calibration**

All three in-situ gas sensors (two identical SO<sub>2</sub>, one CO<sub>2</sub>) were calibrated using test gas standards mixed with nitrogen, using either Tedlar bags, dynamic dilution or readily mixed test gases. The sensors were exposed to different mixing ratios by pumping the gas mixes through the system. Calibration functions were fitted, including errors in mixing ratio and signal (York et al., 2004) to give sensitivities (slope) and offset levels (intercept) (Supplementary Material Fig. S2 – S4). As the CO<sub>2</sub> sensor responds to the gas concentration (molecules per volume), CO<sub>2</sub> mixing ratios (molecules per molecules of air) were obtained by compensating the concentration signals with pressure and temperature data recorded by the built in sensors, assuming ideal gas behavior. The SO<sub>2</sub> sensor output however, relates directly to the mixing ratio, due to the diffusivity of the transport

membrane being inversely proportional to the pressure and therefore cancelling out the pressure dependency of the concentration. The two gas sensors operate with significantly different response times ( $T_{90}$  for  $\text{CO}_2 \sim 2$  s, for  $\text{SO}_2 \sim <20$  s), since sample gas enters the  $\text{SO}_2$  sensor only by molecular diffusion, whereas in the  $\text{CO}_2$  sensor it is directly driven through the optical cell. In order to adjust the response times of the two sensors, a slow response signal for the  $\text{CO}_2$  sensor ( $\text{CO}_{2,\text{sim}}$ ) was 5 simulated. This was achieved through convolution of the original signal with a typical sensor pulse response

$$f(t) = \begin{cases} 0, & t < 0 \\ \frac{1}{\tau} e^{-t/\tau}, & t \geq 0 \end{cases}$$

with  $t$  being time and  $\tau$  being the ‘response time factor’, which in this context can be regarded as a measure for the degree of smoothing. The approach is mathematically equivalent to an approach shown by Roberts et al. (2014). The response time factor  $\tau$  was tuned, such that the correlation of  $\text{CO}_{2,\text{sim}}$  and  $\text{SO}_2$  signal got maximized for discrete peaks (see Fig. 5 (a)). This was 10 already done by Arellano et al. (2017), who also applied the Sunkist instrument in gas measurements in Papua New Guinea in 2016.

### 3.5.2 Gas diffusion denuder analysis

The sampled gas diffusion denuders were sealed air tight and stored in darkness for subsequent analysis. The coating, which contained the derivate and derivatization agent in excess (TMB or EP), was eluted off the denuders using 5 times 2 mL of 1:1 15 of ethyl acetate and ethanol (in case of TMB) or 5 times 2 mL methanol (EP). After the elution, the solvent was evaporated (at 35 °C under gentle  $\text{N}_2$  gas stream) to a volume of approximately 100  $\mu\text{L}$ . Internal standards (with TMB: 2,4,6-tribromoaniline; with EP: neocuproine) were added to each sample solution to account for evaporation losses. The condensed samples were analyzed by GC-MS (TMB) and LC-MS (EP) and quantified using external calibration. Due to the lack of a pure calibration 20 standard hydrogen bromide was only measured qualitatively. Halogen mixing ratios in air were derived from the measured halogen amounts on the denuders and the respective sampling volume obtained by the sampling pump data. In addition to the actual sample denuders open field blank denuders were prepared to account for potential diffusive gas precipitation during the flights.

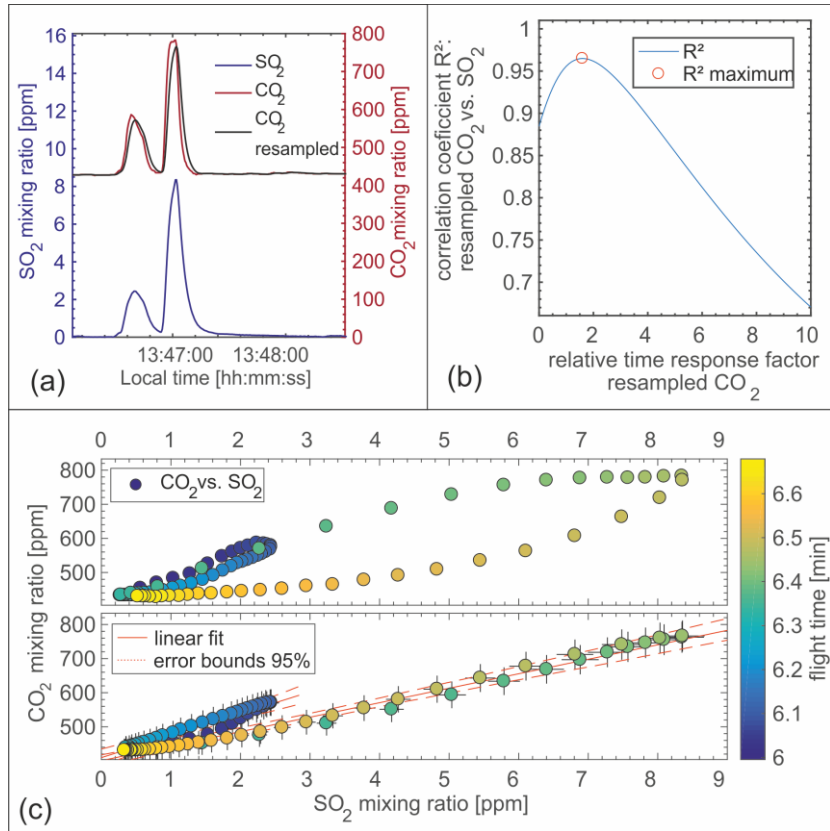
### 3.5.3 Gas ratios

For a feasible data interpretation, gas ratios were calculated from the sensor data and the denuder analysis results. Halogen 25 mixing ratios were interpreted concerning dilution with ambient air by relating to  $\text{SO}_2$ , which is rather slow in its oxidation, and therefore can be treated as a stable dilution proxy for a short term plume observation (Porter et al., 2002). Thus, the derived halogen mixing ratio was divided by the time-integrated  $\text{SO}_2$  mixing ratios obtained during the denuder sampling period to obtain  $\text{BrX}/\text{SO}_2$  ratios. Due to a baseline drift in the  $\text{CO}_2$  sensor data, which was only observable during long-term 30 measurements ( $> 45$  minutes), the pressure and time-response corrected  $\text{CO}_2$  data was additionally drift corrected for long-term measurements. To do so, a linear fit was made to the sloped background signal and subtracted from the  $\text{CO}_2$  signal (see

supplementary material Fig. S5).  $\text{CO}_2/\text{SO}_2$  ratios were calculated with a linear fit to  $\text{CO}_2$  vs.  $\text{SO}_2$  scatter plots, considering the deviations (York et al., 2004) of the two sensor signals.

### 3.5.4 DROAS evaluation and gas fluxes

$\text{SO}_2$  emission rates during the flights at Turrialba were derived by traversing the plume with the DROAS instrument pointing vertically upwards in the direction of the plume. The “mobile DOAS” software developed at Chalmers University was used to control the spectrometer and to retrieve  $\text{SO}_2$  column amounts from the spectra. The  $\text{SO}_2$  columns were achieved using a wavelength evaluation window of 310-330 nm and including  $\text{O}_3$  and  $\text{SO}_2$  absorption cross sections convoluted with a slit function as well as a Ring Spectrum and a 3<sup>rd</sup> order polynomial in the DOAS fitting routine. The calculation of the  $\text{SO}_2$  emission rate involves the integration of the  $\text{SO}_2$  column amounts measured along the flight path resulting in a cross-sectional  $\text{SO}_2$  area, which was geometrically corrected to obtain a surface that is orthogonal to the plume direction, and then multiplied by the wind speed (obtained from the NOAA National Center for Environmental Predictions (NCEP) Global Forecast System) to calculate  $\text{SO}_2$  fluxes. Further details on the spectral evaluation routines and flux calculations can be found elsewhere (de Moor et al., 2017).



5 **Figure 5: (a) Example of time series for mixing ratios of SO<sub>2</sub> and CO<sub>2</sub> (original data in red, resampled data in black), showing discrete gas masses at Stromboli volcano (1st flight on 05th April 2016), (b) Correlation plot for the determination of the relative time response factor for the CO<sub>2</sub> gas sensor with a maximum at a relative time response factor of 1.7, (c) CO<sub>2</sub> over SO<sub>2</sub> mixing ratios, showing the outcome of the resampling of the fast CO<sub>2</sub> with a relative time response factor of 1.7 (lower plot), linear regression results CO<sub>2</sub>/SO<sub>2</sub> ratios of 64 ± 16 the first peak and 42 ± 4 for the second.**

## 4. Results and discussion

### 4.1. Multicopter performance assessment

During the deployment at three volcanoes, the RAVEN multicopter conducted more than 50 flights under moderate wind conditions, in most cases below 10 m/s. The multicopter achieved a maximum operation altitude of 3320 m at Turrialba volcano and records showed a maximum speed of 85 km/h. With a takeoff weight of 2.45 kg and a payload of maximum 1.3 kg flights at Turrialba volcano were still possible, although the flight time was reduced to about 5 to 8 minutes. At the Masaya volcano sites (takeoff altitude ~ 500 m), a maximum ascent above ground level of 1080 m was recorded. A typical flight time at this site was between 10 and 15 minutes. The telemetrically transmitted SO<sub>2</sub> mixing ratios from the Black Box apparatus allowed the localization of high plume densities and therefore adjustments on the optimal hover location. While flying in the line of sight the system could be reliably controlled within a distance of 1-2 km to the operator. However, entering the dense plume proved to challenge the connection between remote control and receiver, resulting in multiple connection losses during flights, in which the UAV also left the line-of-sight of the operator. Nevertheless, GPS connection was still present and an automated return mechanism allowed regaining control after the UAV left areas of high plume densities. At Masaya this phenomenon was observed mostly in a plume with condensed water and SO<sub>2</sub> mixing ratios in low one-digit ppmv numbers, while in a plume without condensation close to the crater control was maintained even with SO<sub>2</sub> levels up to 40 ppmv. This is probably due to the attenuation effect of fog and cloud droplets on millimeter-waves, as they are used with the 2.4 Ghz transmitter of the remote control (Zhao and Wu, 2000).

### 4.2 CO<sub>2</sub>/SO<sub>2</sub> gas sensors

25 During two field deployments at Stromboli (Table 2) and Masaya (Table 3) volcanoes, the lightweight gas monitoring system Sunkist (SK) determined CO<sub>2</sub>/SO<sub>2</sub> gas ratios at various airborne and ground-based locations. A comparison with a stationary Multi-GAS (MG) instrument at Masaya volcano for the same site and time (lookout point south, 14<sup>th</sup> July 2016, 11:19) and with inlets of both systems in proximity to each other gave results on CO<sub>2</sub>/SO<sub>2</sub> ratios that were within each other's 2-sigma intervals (CO<sub>2</sub>/SO<sub>2</sub> of 2.9 ± 0.3 for MG and 3.6 ± 0.4 for SK). The time series of the SO<sub>2</sub> mixing ratios of SK and MG also showed a good agreement ( $R^2 = 0.89$ ) (Fig. 6). An application of SK further downwind (0.5 km from the rim) gave a CO<sub>2</sub>/SO<sub>2</sub> ratio of 3.3 ± 1.2, while the MG measured a CO<sub>2</sub>/SO<sub>2</sub> ratio of 3.1 ± 0.1 during the same time at the rim. This is showing SK's ability for deployment in a more diluted plume, although with the disadvantage of higher errors, due to the higher relative background in CO<sub>2</sub> at more distant locations. Furthermore, UAV-based application (9 flights, 17<sup>th</sup> – 20<sup>th</sup> July 2017) between

1.5 km and 2 km downwind of the Masaya plume resulted in average 42 % higher CO<sub>2</sub>/SO<sub>2</sub> ratios with a larger standard deviation compared to the crater rim (14<sup>th</sup> – 16<sup>th</sup> July 2017), but still within each other's errors (CO<sub>2</sub>/SO<sub>2</sub>: 5.4 ± 2.3 at 1.5 - 2 km; 3.8 ± 0.3 at the rim). Due to the limitations of the CO<sub>2</sub> sensing, acquirement of useful CO<sub>2</sub>/SO<sub>2</sub> data with SK is more feasible in dense plumes close to, but not limited to the crater rim, as the airborne application has shown. Additionally, SO<sub>2</sub> mixing ratios were measured as a plume dilution proxy by the Black Box (BB) system. Both the BB and SK systems use an identical SO<sub>2</sub> sensor and showed a good agreement of their SO<sub>2</sub> time series and time integrated SO<sub>2</sub> mixing ratio (SK: 1.75 ± 0.08 ppmv, BB: 1.84 ± 0.08 ppmv) (supplement material S6).

At Stromboli volcano, the Sunkist and Black Box systems were deployed on two days (05<sup>th</sup> & 06<sup>th</sup> April 2016), resulting in seven flights into the plume. These flights covered distances of between 11 m and 419 m from the vent in a downwind direction (northeast), above the Sciara del Fuoco. As shown in Figure 1, discrete gas clouds with different CO<sub>2</sub>/SO<sub>2</sub> compositions were measured. The retrieved CO<sub>2</sub>/SO<sub>2</sub> ratios ranged between 7 and 64, with the higher values typically detected directly above the vent (11 m to 26 m) (see Tab. 3 and Fig. 1). During the multicopter operations close to the vent regular strombolian ash explosions occurred (see Fig. 3 (d) and (e)), which are likely accompanied by CO<sub>2</sub>-rich gas clouds (La Spina et al., 2013) and therefore act as a possible explanation for the detected high CO<sub>2</sub>/SO<sub>2</sub> ratios. On both flight days the predominant wind direction was southwest (207° ± 15° and 210° ± 18°, data from weather station at 77 m a.s.l., commercially available from [windfinder.com](http://windfinder.com), Kiel, Germany), which resulted in the plume mostly being present across the Sciara del Fuoco and therefore only accessible by UAV. Nevertheless, a local Multi-GAS station (placed on the SE rim of the crater terrace) discontinuously measured the plume during the period of the UAV survey, showing CO<sub>2</sub>/SO<sub>2</sub> ratios between 2.2 and 13.6, which is in agreement with some of the multicopter-based measurements. Similar CO<sub>2</sub>/SO<sub>2</sub> ratios have been observed in the past and are exemplary for ordinary Strombolian activity (Aiuppa et al., 2009). It has to be taken into account that both instruments did not measure simultaneously or in proximity to each other. The MG instrument only measures twice a day for 30 minutes and averages over this time, while with the SK instrument we identified discrete peaks of gas clouds with different CO<sub>2</sub>/SO<sub>2</sub> ratios. Furthermore, a comparison of SK and MG CO<sub>2</sub>/SO<sub>2</sub> data might be more accurate with the high SK CO<sub>2</sub>/SO<sub>2</sub> values (associated with eruptive degassing) left aside, as we lack the observations on passive, respectively eruptive degassing behavior for the MG data records.

25

**Table 2: Overview on the retrieved CO<sub>2</sub>/SO<sub>2</sub> ratios with parameters for the linear fit at Stromboli volcano**

| Date  | Time  | Flight / Peak | CO <sub>2</sub> /SO <sub>2</sub> | lower SO <sub>2</sub> limit /ppmv | Data Points | max. SO <sub>2</sub> /ppmv | estimated distance /m |
|-------|-------|---------------|----------------------------------|-----------------------------------|-------------|----------------------------|-----------------------|
| 05.04 | 13:46 | 1 / 1         | 64 ± 16                          | 1                                 | 39          | 2.6                        | 26                    |
| 05.04 | 13:46 | 1 / 2         | 42 ± 4                           | 1                                 | 48          | 8.5                        | 11                    |
|       |       |               |                                  |                                   |             |                            |                       |
| 05.04 | 14:31 | 2 / 1         | 43 ± 8                           | 1                                 | 31          | 4.5                        | 18                    |
| 05.04 | 14:32 | 2 / 2         | 31 ± 12                          | 1                                 | 29          | 4.7                        | 25                    |
| 05.04 | 16:18 | 3 / 1         | 7 ± 5                            | 0.1                               | 101         | 5.8                        | 419                   |

|       |       |       |         |     |     |     |     |
|-------|-------|-------|---------|-----|-----|-----|-----|
| 05.04 | 16:23 | 3 / 2 | 11 ± 11 | 0.1 | 133 | 1.9 | 399 |
| 06.04 | 13:03 | 4 / 1 | 27 ± 25 | 0.2 | 326 | 0.9 | 155 |
| 06.04 | 13:44 | 5 / 1 | 22 ± 5  | 0.5 | 324 | 5.2 | 80  |
| 06.04 | 14:44 | 6 / 1 | 10 ± 13 | 0.2 | 111 | 1.6 | 170 |
| 06.04 | 14:45 | 6 / 2 | 21 ± 7  | 0.5 | 415 | 2.3 | 177 |
| 06.04 | 15:10 | 7 / 1 | 9 ± 5   | 0.2 | 516 | 1.6 | 167 |
| 06.04 | 15:16 | 7 / 2 | 21 ± 5  | 0.5 | 35  | 2.3 | 107 |

Table 3: CO<sub>2</sub>/SO<sub>2</sub> mixing ratios and calculation parameters obtained from the Sunkist (SK) and Multi-GAS (MG) instrument at Masaya Volcano. The exact locations are given in Fig 2, errors indicate 2 sigma interval (95.5 %) retrieved by a linear regression (York et al., 2004) including the measurement errors of both the SO<sub>2</sub> (error: 5-10 %) and CO<sub>2</sub> (error: 5.5 %) sensor

| Date       | Time          | Instrument | Location / Flight           | CO <sub>2</sub> /SO <sub>2</sub> | lower SO <sub>2</sub> limit /ppmv | Data Points | max. SO <sub>2</sub> | distance to rim /km |
|------------|---------------|------------|-----------------------------|----------------------------------|-----------------------------------|-------------|----------------------|---------------------|
| 14.07.2016 | 09:43 - 15:10 | MG         | Santiago rim; lookout south | 2.9 ± 0.1                        | 4                                 | 3200        | 31.1                 | 0                   |
| 14.07.2016 | 11:18 - 11:44 | MG         | Santiago rim; lookout south | 2.9 ± 0.3                        | 4                                 | 440         | 17.5                 | 0                   |
| 14.07.2016 | 11:19 - 11:45 | SK         | Santiago rim; lookout south | 3.8 ± 0.5                        | 4                                 | 1460        | 17.9                 | 0                   |
| 14.07.2016 | 10:42 - 12:09 | SK         | Santiago rim; lookout south | 3.6 ± 0.4                        | 4                                 | 2600        | 18.5                 | 0                   |
| 15.07.2016 | 09:43 - 16:23 | MG         | Santiago rim; pole site     | 3.1 ± 0.1                        | 4                                 | 2950        | 29.6                 | 0                   |
| 15.07.2016 | 15:28 - 16:19 | SK         | Nindiri rim                 | 3.3 ± 1.2                        | 1                                 | 3100        | 5.8                  | 0.5                 |
| 16.07.2016 | 11:18 - 12:19 | SK         | Santiago rim; pole site     | 4.7 ± 0.3                        | 4                                 | 3000        | 28                   | 0                   |
| 17.07.2016 | 08:56 - 08:59 | SK         | caldera valley; flight #A2  | 2.9 ± 13                         | 1                                 | 150         | 2.8                  | 1.8                 |
| 17.07.2016 | 11:21 - 11:28 | SK         | caldera valley; flight #A5  | 4.8 ± 3.2                        | 1                                 | 630         | 4.8                  | 1.8                 |
| 17.07.2016 | 11:53 - 12:01 | SK         | caldera valley; flight #A6  | 6.5 ± 3.4                        | 0.2                               | 620         | 3.4                  | 1.9                 |
| 17.07.2016 | 12:10 - 12:20 | SK         | caldera valley; flight #A7  | 6.2 ± 5.6                        | 0.4                               | 1150        | 2.2                  | 1.5                 |
| 18.07.2016 | 07:55 - 09:36 | SK         | Santiago rim; pole site     | 4.1 ± 0.3                        | 4                                 | 4350        | 36.7                 | 0                   |
| 18.07.2016 | 13:19 - 13:27 | SK         | caldera valley; flight #B4  | 5.1 ± 4                          | 1                                 | 560         | 4.4                  | 1.7                 |
| 20.07.2016 | 12:55 - 13:04 | SK         | caldera valley; flight #C1  | 7.5 ± 5.8                        | 0.5                               | 310         | 2.8                  | 1.9                 |
| 20.07.2016 | 13:29 - 13:35 | SK         | caldera valley; flight #C2  | 7.7 ± 5.1                        | 0.75                              | 470         | 2.9                  | 1.9                 |
| 20.07.2016 | 13:58 - 14:07 | SK         | caldera valley; flight #C3  | 2.2 ± 11                         | 0.5                               | 380         | 1.9                  | 1.9                 |
| 20.07.2016 | 16:22 - 16:29 | SK         | caldera valley; flight #C7  | 5.3 ± 4.4                        | 0.5                               | 550         | 3.4                  | 2                   |

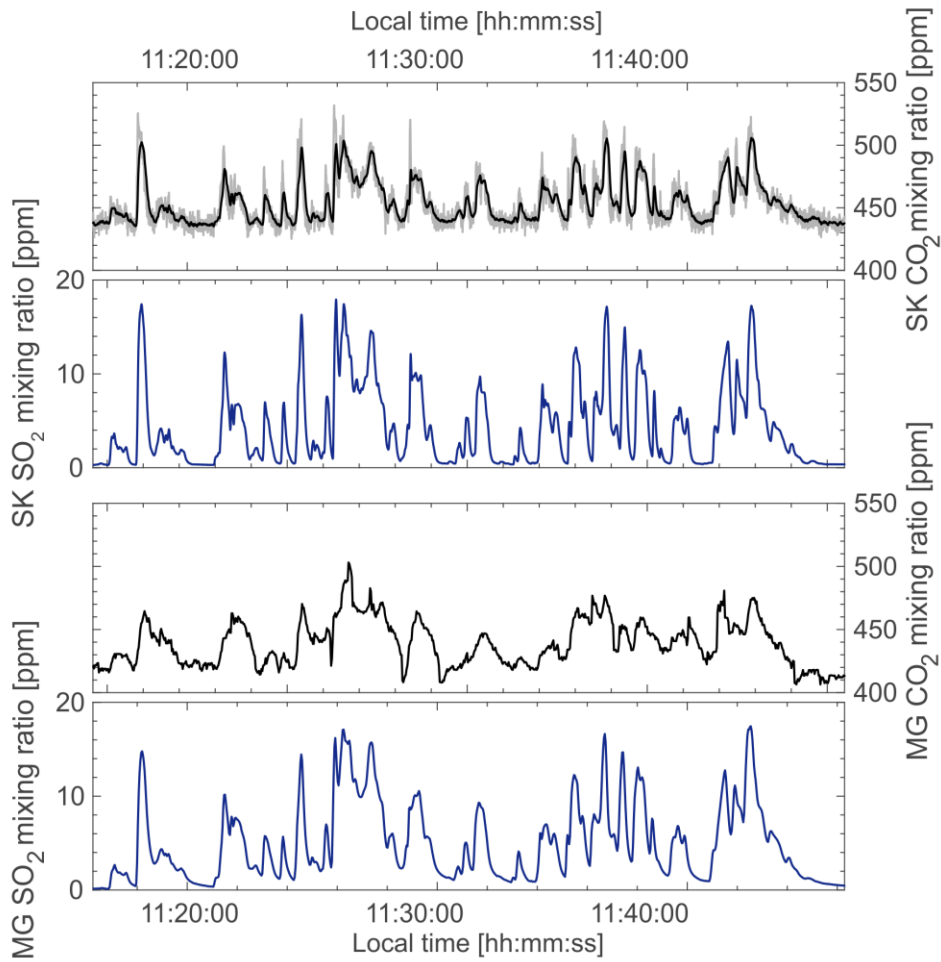


**Figure 6: Comparison of SO<sub>2</sub> and CO<sub>2</sub> time series of a Multi-GAS (MG) instrument and the *Sunkist* (SK) unit at the Masaya volcano crater rim (for SK CO<sub>2</sub> raw data in grey, resampled data in black), both instruments inlets were place in proximity to each other (14<sup>th</sup> July 2016); SK CO<sub>2</sub>/SO<sub>2</sub> = 3.63+/- 0.43 background CO<sub>2</sub> = 439 ppm); MG CO<sub>2</sub>/SO<sub>2</sub> = 2.94 +/- 0.30 (background CO<sub>2</sub> = 413 ppm); (additional scatter plots in the supplementary material)**

5

#### 4.3 Halogen measurements

Bromine species were detected by gas diffusion denuder sampling on three of the seven flights at Stromboli volcano. Reactive bromine species were measured between 0.14 and 0.65 ppb (see Table 4), while HBr was determined qualitatively in all three samples.

10 The obtained ratios of reactive bromine (BrX) to SO<sub>2</sub> ( $1.9 \times 10^{-4}$  –  $9.8 \times 10^{-4}$ ) are within the range of bromine to sulfur ratios produced by other methods at Stromboli volcano, e.g. alkaline trap sampling by Wittmer et al. (Wittmer et al., 2014) ( $4.3 \times 10^{-4}$  –  $2.36 \times 10^{-2}$ ). Figure 7 (b) shows the BrX/SO<sub>2</sub> ratios for different plume ages, which was calculated by taking wind speeds into account. Although the general feasibility of the used methods for the investigation of reactive halogen species in an aging

plume is demonstrated in this proof-of-principle approach, a trend in the BrX/SO<sub>2</sub> ratio over age is not recognizable for this limited data set. Without information on abundances of other halogen species such as BrO<sub>(g)</sub>, HBr<sub>(g)</sub> and aqueous particulate bromine (HBr<sub>(aq)</sub>), interpretation of the BrX/SO<sub>2</sub> ratio is difficult as the emitted gas composition may also change on shorter time scales (La Spina et al., 2013) compared to the campaign duration. However, an increase of the reactive bromine species 5 BrO with distance from the crater rim has been observed previously by DOAS measurements at various volcanoes and is well described in the literature (Oppenheimer et al., 2006; Bobrowski et al., 2007). Although the bromine speciation in volcanic plumes has been subject of several ground-based (e.g. Gliß et al., 2015) airplane (e.g. General et al., 2015), satellite (e.g. Theys et al., 2009; Hörmann et al., 2013) and model studies (e.g. Bobrowski et al., 2007; Roberts et al., 2009; von Glasow, 2010; 10 Roberts et al., 2014; Jourdain et al., 2016) in recent years, in-situ measurements are scarce. The data presented here for the first minute after emission highlight the potential of UAV-based measurements to improve sample acquisition and thus obtain 15 a better understanding of plume aging.

As shown in Figure 7 (c), the BrX to SO<sub>2</sub> ratio seems to change not only with the plume age but also with CO<sub>2</sub>/SO<sub>2</sub> mixing ratios, which were simultaneously measured. However, with only three data points a further interpretation is inadequate due to lack of a statistical basis. Nevertheless, these first results show the principal practicality of the used denuder sampling and 15 gas sensing methods for simultaneous investigation of halogen, carbon and sulfur emissions.

**Table 4: Sample parameter and bromine measurement results for three denuder samples at Stromboli volcano.**

| Sample number                              | 1           | 2           | 3           |
|--|-------------|-------------|-------------|
| <b>Date</b>                                | 05.04.2016  | 06.04.2016  | 06.04.2016  |
| <b>Time</b>                                | 14:31       | 13:46       | 14:45       |
| <b>Duration /s</b>                         | 53          | 364         | 320         |
| <b>Sample volume /L</b>                    | 0.18        | 1.26        | 1.11        |
| <b>pressure /mbar</b>                      | 906         | 914         | 914         |
| <b>integrated SO<sub>2</sub>/ppmv</b>      | 1.85 ± 0.09 | 0.34 ± 0.04 | 0.74 ± 0.05 |
| <b>BrX /ppb</b>                            | 0.65 ± 0.06 | 0.34 ± 0.01 | 0.14 ± 0.1  |
| <b>BrX/SO<sub>2</sub> *10<sup>-4</sup></b> | 3.5 ± 0.4   | 9.8 ± 1.3   | 1.9 ± 0.2   |
| <b>CO<sub>2</sub>/SO<sub>2</sub></b>       | 43 ± 9      | 27 ± 4      | 17 ± 8      |
| <b>distance /m</b>                         | 21 ± 2      | 80 ± 2      | 177 ± 2     |
| <b>wind speed /m s<sup>-1</sup></b>        | 3.4 ± 0.5   | 4.8 ± 0.5   | 4.8 ± 0.5   |
| <b>plume age /s</b>                        | 6 ± 1       | 17 ± 2      | 37 ± 4      |

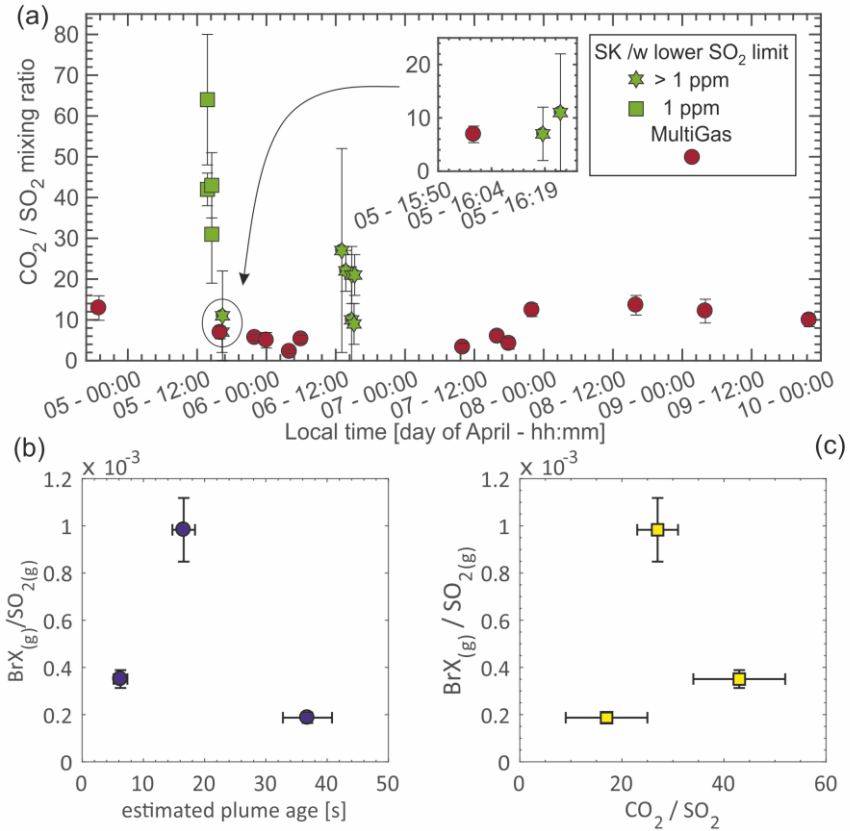


**Figure 7: (a) Measured CO<sub>2</sub>/SO<sub>2</sub> gas ratios over a 5-day period by a Multi-GAS station (located east of the crater terrace) and airborne measurements with the *Sunkist* system at Stromboli volcano, data point shapes indicate the lower SO<sub>2</sub> mixing ratio limits for the linear fit over the CO<sub>2</sub> vs SO<sub>2</sub> data, (b) development of the gaseous reactive bromine species over SO<sub>2</sub> over the estimated plume age (derived from distance to crater and estimated wind speed), (c) gaseous reactive bromine/SO<sub>2</sub> ratios vs. CO<sub>2</sub>/SO<sub>2</sub> ratio**

5

#### 4.4. DROAS measurements

On September 27<sup>th</sup>, two DROAS plume transects were performed at Turrialba volcano during mild ash emission at around 2800 m a.s.l. with a total flight time of approximately 10 minutes. The flight was conducted in the downwind direction west of the active vent and crossed underneath the plume on a south-north axis (Fig. 8 (b)), exiting the plume on both ends of the 10 flight path, which is indicated by the low SO<sub>2</sub> column amounts close to the baseline in the northern- and southern-most section of the flightpath (Fig. 8 (c)). SO<sub>2</sub> fluxes were calculated for that flight and resulted in  $1776 \pm 1108$  T/d SO<sub>2</sub> for traverse A and  $1616 \pm 1007$  T/d SO<sub>2</sub> for traverse B (see Table 5). Calculation of the SO<sub>2</sub> fluxes obtained by the two scanning DOAS instrument from the NOVAC network, located on the southern edge of the plume, gave average results of  $1533 \pm 986$  T/d SO<sub>2</sub> for *La Silva* and  $1094 \pm 704$  T/d SO<sub>2</sub> from *La Cetral* for a 2-hour period, in which the flight took place. Therefore, the results 15 of the DROAS traverses are in a good agreement with the scanning DOAS stations. De Moor et al. (de Moor et al., 2016a) conducted car based mobile DOAS transects, which typically take ~45 minutes for a round trip due to rough terrain. Dynamic gas plumes can significantly change the plume's travel direction on scales of minutes, introducing a significant source of error

to car traverses. A major advantage of the UAV method is that it is much quicker, about 10 minutes for a round trip, thus providing a more accurate snapshot of the plume.

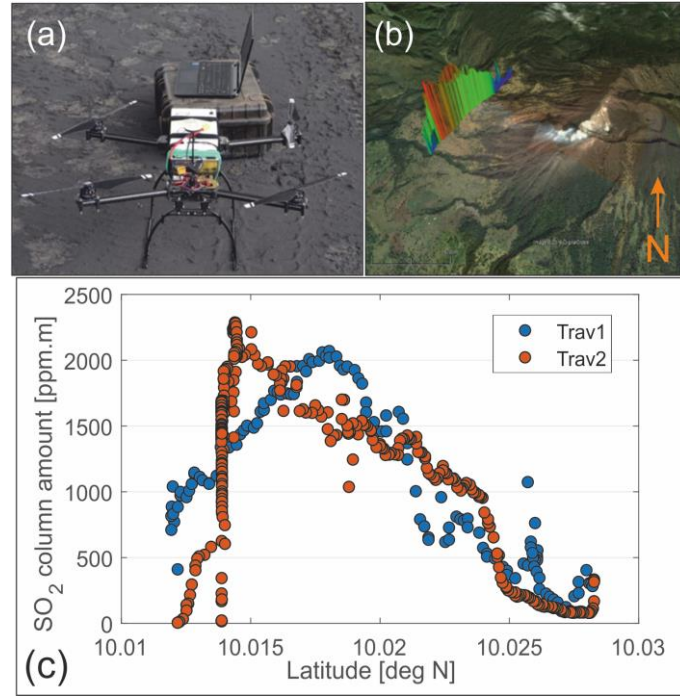


Figure 8: (a) Drone-operated miniature DOAS setup, (b) Illustration of SO<sub>2</sub> column amounts measured by DROAS at Turrialba volcano, (c) SO<sub>2</sub> column amounts during the transversal flight underneath the plume

Table 5: SO<sub>2</sub> fluxes obtained by DROAS traverses and two stationary scanning DOAS instruments at Turrialba volcano. The average fluxes from La Silva and La Central were derived for a 2-hour period in which the DROAS flights were conducted, maximum fluxes for this period as presented as well

| Instrument/Traverse              | SO <sub>2</sub> flux at 1 m/s |        | error | windspeed | SO <sub>2</sub> flux |             |
|----------------------------------|-------------------------------|--------|-------|-----------|----------------------|-------------|
| [unit]                           | [T/d]                         |        | [%]   | [m/s]     | [T/d]                |             |
| DROAS Traverse A                 | 419.9                         | ± 38.6 | 9.2   | 3.78      | ± 2.62               | 1776 ± 1108 |
| DROAS Traverse B                 | 381.6                         | ± 35.5 | 9.3   | 3.78      | ± 2.62               | 1614 ± 1007 |
| La Silvia NOVAC station AVERAGE  | 362.3                         | ± 72.5 | 20    | 3.78      | ± 2.62               | 1533 ± 986  |
| La Silvia NOVAC station MAX      | 481.72                        | ± 96.3 | 20    | 3.78      | ± 2.62               | 2038 ± 1312 |
| La Central NOVAC station AVERAGE | 258.6                         | ± 51.7 | 20    | 3.78      | ± 2.62               | 1094 ± 704  |
| La Central NOVAC station MAX     | 448.1                         | ± 89.6 | 20    | 3.78      | ± 2.62               | 1896 ± 1220 |

## 5. Conclusion and outlook

In this study we have demonstrated the feasibility of a multicopter-based approach for volcanic in-situ plume measurements to achieve investigations on the compositional variability of an aging plume. The use of a multicopter UAV proved to be a suitable alternative to ground-based operations, especially in hard to access or not at all accessible areas, like active volcanic

5 vents or elevated downwind plumes. The aerial sampling systems demonstrated robustness and effectiveness during the field missions with harsh environmental and meteorological conditions, including ash-laden plumes. With the newly developed sampling system, reactive halogen species were observable in previously inaccessible downwind plume areas. Halogen speciation information enhances our understanding of plume chemistry in the aging plume, which represents important knowledge for new volcano monitoring approaches. Therefore, in-situ speciation methods for halogens should be extended  
10 and optimized for other gaseous and aqueous compounds including chlorine and iodine species. Additionally, at Stromboli volcano changes in the BrX/SO<sub>2</sub> ratios were observed with different CO<sub>2</sub>/SO<sub>2</sub> ratios, which represents an interesting matter and should be further explored in future studies.

Furthermore, multicopter-based CO<sub>2</sub>/SO<sub>2</sub> ratio measurements showed its reliability, opening a promising approach for monitoring inaccessible volcanoes or during dangerous eruptions minimizing personnel risk at highly active volcanoes.

15 Although we demonstrated the applicability of the Sunkist lightweight gas sensing system for potential UAV based monitoring, challenges in the acquisition of high-quality data for diluted plumes still exist. Thus, more sophisticated components (e.g. sensors, microcontroller or data logger) promise to achieve better sensitivities, but with the disadvantage of higher losses in the case of a crash.

Moreover, the herein presented UAV application of a miniature DOAS instrument (DROAS) for SO<sub>2</sub> gas flux measurements  
20 has shown its quality in the harsh environment of Turrialba volcano. The potential to be an excellent alternative to walking or car-based traverses for SO<sub>2</sub> flux acquisition has been proven with a significant reduction of risks and operation time.

The case studies presented here explored the general feasibility of multirotor UAVs in volcanic plume studies and are an initial step in the direction of remotely operated gas measurements at active volcanoes. We have shown the potential of UAV-based sampling to gain insights into reactive halogen chemistry and processes of plume aging, and further application of this method  
25 could yield data from previously unstudied plume regions. Technological advances promise to enable scheduled pre-programmed and autonomous UAV operations (e.g. from hangars close to volcanoes) with extended flight times for regular hazard assessments.

## Competing interests

30 The authors declare that they have no conflict of interest.

## Acknowledgements

Julian Rüdiger, Nicole Bobrowski, Alexandra Gutmann and Thorsten Hoffmann acknowledge support by the research center 'Volcanoes and Atmosphere in Magmatic, Open Systems' (VAMOS), University of Mainz, Germany. Julian Rüdiger is thankful for funding from Max Planck Graduate School at the MPIC (MPGS), Mainz, the German Academic Exchange Service 5 (DAAD) and the support by OVSICORI (Costa Rica) and INETER (Nicaragua). The authors also thank Ulrich Platt for his support on the theoretical assessment of multicopter sampling and Christoph Kern for reviewing and improving the manuscript.

## References

10 Aiuppa, A., Federico, C., Giudice, G., Gurrieri, S., Liuzzo, M., Shinohara, H., Favara, R., and Valenza, M.: Rates of carbon dioxide plume degassing from Mount Etna volcano, *J. Geophys. Res.-Sol. Ea.*, 111, B9, doi:10.1029/2006JB004307, 2006.

15 Aiuppa, A., Moretti, R., Federico, C., Giudice, G., Gurrieri, S., Liuzzo, M., Papale, P., Shinohara, H., and Valenza, M.: Forecasting Etna eruptions by real-time observation of volcanic gas composition, *Geol.*, 35, 12, doi:10.1130/G24149A.1, 2007.

20 Aiuppa, A., Federico, C., Giudice, G., Giuffrida, G., Guida, R., Gurrieri, S., Liuzzo, M., Moretti, R., and Papale, P.: The 2007 eruption of Stromboli volcano: Insights from real-time measurement of the volcanic gas plume CO<sub>2</sub>/SO<sub>2</sub> ratio, *J. Volcanol. Geotherm. Res.*, 182, 221–230, doi:10.1016/j.jvolgeores.2008.09.013, 2009.

25 Aiuppa, A., Fischer, T. P., Plank, T., Robidoux, P., and Di Napoli, R.: Along-arc, inter-arc and arc-to-arc variations in volcanic gas CO<sub>2</sub>/ST ratios reveal dual source of carbon in arc volcanism, *Earth-Sci. Rev.*, 168, 24–47, doi:10.1016/j.earscirev.2017.03.005, 2017.

30 Allard, P., Carbonnelle, J., Dajlevic, D., Le Bronec, J., Morel, P., Robe, M. C., Maurenas, J. M., Faivre-Pierret, R., Martin, D., Sabroux, J. C., and Zettwoog, P.: Eruptive and diffuse emissions of CO<sub>2</sub> from Mount Etna, *Nature*, 351, 387–391, doi:10.1038/351387a0, 1991.

35 Allard, P., Aiuppa, A., Burton, M., Caltabiano, T., Federico, C., Salerno, G., and La Spina, A.: Crater gas emissions and the magma feeding system of Stromboli volcano, in *The Stromboli Volcano: An Integrated Study of the 2002-2003 Eruption*, (eds S. Calvari, S. Inguaggiato, G. Puglisi, M. Ripepe and M. Rosi), American Geophysical Union, Washington, D. C., 65–80, doi: 10.1029/182GM07, 2008.

40 Altstädter, B., Platis, A., Wehner, B., Scholtz, A., Wildmann, N., Hermann, M., Käthner, R., Baars, H., Bange, J., and Lampert, A.: ALADINA – an unmanned research aircraft for observing vertical and horizontal distributions of ultrafine particles within the atmospheric boundary layer, *Atmos. Meas. Tech.*, 8, 1627–1639, doi:10.5194/amt-8-1627-2015, 2015.

45 Alvarado, M., Gonzalez, F., Erskine, P., Cliff, D., and Heuff, D.: A Methodology to Monitor Airborne PM10 Dust Particles Using a Small Unmanned Aerial Vehicle, *Sensors*, 17, 343, doi:10.3390/s17020343, 2017.

50 Arellano, S., Galle B., Mulina K., Wallius, J., McCormick, B., Salem, L., D'aleo, R., Itikarai I., Tirpitz, L., Bobrowski, N., and Aiuppa, A.: Recent observations of carbon and sulfur gas emissions from Tavurvur, Bagana and Ulawun (Papua New Guinea) with a combination of ground and air-borne direct and remote sensing techniques, Abstract EGU2017-13644 presented at 2017 General Assembly, EGU, Vienna, Austria, 23-28 April.

55 Bobrowski, N. and Giuffrida, G.: Bromine monoxide/sulphur dioxide ratios in relation to volcanological observations at Mt. Etna 2006-2009, *Solid Earth*, 3, 433–445, 2012.

60 Bobrowski, N., Glasow, R. von, Aiuppa, A., Inguaggiato, S., Louban, I., Ibrahim, O. W., and Platt, U.: Reactive halogen chemistry in volcanic plumes, *J. Geophys. Res.*, 112, doi:10.1029/2006JD007206, 2007.

65 Bobrowski, N., Giuffrida, G. B., Arellano, S., Yalire, M., Liotta, M., Brusca, L., Calabrese, S., Scaglione, S., Rüdiger, J., Castro, J. M., Galle, B., and Tedesco, D.: Plume composition and volatile flux of Nyamulagira volcano, Democratic

Republic of Congo, during birth and evolution of the lava lake, 2014–2015, *Bull Volcanol.*, 79, B09207, doi:10.1007/s00445-017-1174-0, 2017.

Burton, M. R., Sawyer, G. M., and Granieri, D.: Deep Carbon Emissions from Volcanoes, *Rev. Mineral. Geochem.*, 75, 323–354, doi:10.2138/rmg.2013.75.11, 2013.

5 Carn, S. A., Fioletov, V. E., McLinden, C. A., Li, C., and Krotkov, N. A.: A decade of global volcanic SO<sub>2</sub> emissions measured from space, *Scientific reports*, 7, 44095, doi:10.1038/srep44095, 2017.

Carroll, M. R. and Holloway, J. R.: Volatiles in Magmas, Washington: Mineralogical Society of America, 1994.

de Moor, J. M., Fischer, T. P., Sharp, Z. D., King, P. L., Wilke, M., Botcharnikov, R. E., Cottrell, E., Zelenski, M., Marty, B., Klimm, K., Rivard, C., Ayalew, D., Ramirez, C., and Kelley, K. A.: Sulfur degassing at Erta Ale (Ethiopia) and 10 Masaya (Nicaragua) volcanoes: Implications for degassing processes and oxygen fugacities of basaltic systems, *Geochem. Geophys. Geosy.*, 14, 4076–4108, doi:10.1002/ggge.20255, 2013.

de Moor, J. M., Aiuppa, A., Avard, G., Wehrmann, H., Dunbar, N., Muller, C., Tamburello, G., Giudice, G., Liuzzo, M., Moretti, R., Conde, V., and Galle, B.: Turmoil at Turrialba Volcano (Costa Rica): Degassing and eruptive processes inferred from high-frequency gas monitoring, *Journal of geophysical research. Solid earth*, 121, 5761–5775, 15 doi:10.1002/2016JB013150, 2016a.

de Moor, J. M., Aiuppa, A., Pacheco, J., Avard, G., Kern, C., Liuzzo, M., Martínez, M., Giudice, G., and Fischer, T. P.: Short-period volcanic gas precursors to phreatic eruptions: Insights from Poás Volcano, Costa Rica, *Earth Planet. Sc. Lett.*, 442, 218–227, doi:10.1016/j.epsl.2016.02.056, 2016b.

20 de Moor, J. M., Kern, C., Avard, G., Muller, C., Aiuppa, A., Saballos A., Ibarra M., LaFemina P., Protti M., Fischer, T. P.: A new sulfur and carbon degassing inventory for the Southern Central American Volcanic Arc: The importance of accurate time-series datasets and possible tectonic processes responsible for temporal variations in arc-scale volatile emissions, *Geochem. Geophys. Geosy.*, doi:10.1002/2017GC007141, 2017.

25 Delmelle, P., Stix, J., Baxter, P., Garcia-Alvarez, J., and Barquero, J.: Atmospheric dispersion, environmental effects and potential health hazard associated with the low-altitude gas plume of Masaya volcano, Nicaragua, *Bull. Volcanol.*, 64, 423–434, doi:10.1007/s00445-002-0221-6, 2002.

Diaz, J. A., Pieri, D., Wright, K., Sorensen, P., Kline-Shoder, R., Arkin, C. R., Fladeland, M., Bland, G., Buongiorno, M. F., Ramirez, C., Corrales, E., Alan, A., Alegria, O., Diaz, D., and Linick, J.: Unmanned aerial mass spectrometer systems for in-situ volcanic plume analysis, *J. Am. Soc. Mass Spectrom.*, 26, 292–304, doi:10.1007/s13361-014-1058-x, 2015.

25 Dinger, F., Bobrowski, N., Warnach, S., Bredemeyer, S., Hidalgo, S., Arellano, S., Galle, B., Platt, U., and Wagner, T.: Periodicity in the BrO/SO<sub>2</sub> molar ratios in the volcanic gas plume of Cotopaxi and its correlation with the Earth tides during the eruption in 2015, *Solid Earth Discuss.*, 1–28, doi:10.5194/se-2017-89, 2017.

Faivre-Pierret, R., Martin, D., and Sabroux, J. C.: Contribution des Sondes Aérolégiques Motorisées à l'Etude de la Physico-Chimie des Panaches Volcaniques, *Bull Volcanol.*, 43, 473–485, doi:10.1007/BF02597686, 1980.

30 Galle, B., Johansson, M., Rivera, C., Zhang, Y., Kihlman, M., Kern, C., Lehmann, T., Platt, U., Arellano, S., and Hidalgo, S.: Network for Observation of Volcanic and Atmospheric Change (NOVAC)—A global network for volcanic gas monitoring: Network layout and instrument description, *J. Geophys. Res.*, 115, 151, doi:10.1029/2009JD011823, 2010.

Galle, B., Oppenheimer, C., Geyer, A., McGonigle, A. J., Edmonds, M., and Horrocks, L.: A miniaturised ultraviolet spectrometer for remote sensing of SO<sub>2</sub> fluxes: A new tool for volcano surveillance, *J. Volcanol. Geotherm. Res.*, 119, 241–254, doi:10.1016/S0377-0273(02)00356-6, 2003.

40 General, S., Bobrowski, N., Pöhler, D., Weber, K., Fischer, C., and Platt, U.: Airborne I-DOAS measurements at Mt. Etna: BrO and OCIO evolution in the plume, *J of Volcanol. Geotherm. Res.*, 300, 175–186, doi:10.1016/j.jvolgeores.2014.05.012, 2015.

Gerlach, T. M.: Volcanic sources of tropospheric ozone-depleting trace gases, *Geochem. Geophys. Geosy.*, 5, doi:10.1029/2004GC0007472004.

45 Giggenbach, W. F.: Variations in the carbon, sulfur and chlorine contents of volcanic gas discharges from White Island, New Zealand, *Bull. Volcanol.*, 39, 15–27, doi:10.1007/BF02596943, 1975.

Glasow, R. v., Bobrowski, N., and Kern, C.: The effects of volcanic eruptions on atmospheric chemistry, *Chemical Geology*, 263, 131–142, doi:10.1016/j.chemgeo.2008.08.020, 2009.

50 Glasow, R. v.: Atmospheric chemistry in volcanic plumes, *P. Natl. Acad. Sci. USA*, 107, 6594–6599, doi:10.1073/pnas.0913164107, 2010.

Gliß, J., Bobrowski, N., Vogel, L., Pöhler, D., and Platt, U.: OCIO and BrO observations in the volcanic plume of Mt. Etna – implications on the chemistry of chlorine and bromine species in volcanic plumes, *Atmos. Chem. Phys.*, 15, 5659–5681, doi:10.5194/acp-15-5659-2015, 2015.

Hörmann, C., Sihler, H., Bobrowski, N., Beirle, S., Penning de Vries, M., Platt, U., and Wagner, T.: Systematic investigation of bromine monoxide in volcanic plumes from space by using the GOME-2 instrument, *Atmos. Chem. Phys.*, 13, 4749–4781, doi:10.5194/acp-13-4749-2013, 2013.

Jourdain, L., Roberts, T. J., Pirre, M., and Josse, B.: Modeling the reactive halogen plume from Ambrym and its impact on the troposphere with the CCATT-BRAMS mesoscale model, *Atmos. Chem. Phys.*, 16, 12099–12125, doi:10.5194/acp-16-12099-2016, 2016.

10 La Spina, A., Burton, M. R., Harig, R., Mure, F., Rusch, P., Jordan, M., and Caltabiano, T.: New insights into volcanic processes at Stromboli from Cerberus, a remote-controlled open-path FTIR scanner system, *J. Volcanol. Geotherm. Res.*, 249, 66–76, doi:10.1016/j.jvolgeores.2012.09.004, 2013.

Lee, C., Kim, Y. J., Tanimoto, H., Bobrowski, N., Platt, U., Mori, T., Yamamoto, K., and Hong, C. S.: High ClO and ozone depletion observed in the plume of Sakurajima volcano, Japan, *Geophys. Res. Lett.*, 32, 2005.

15 Liotta, M., Rizzo, A. L., Barnes, J. D., D'Auria, L., Martelli, M., Bobrowski, N., and Wittmer, J.: Chlorine isotope composition of volcanic rocks and gases at Stromboli volcano (Aeolian Islands, Italy): Inferences on magmatic degassing prior to 2014 eruption, *J. Volcanol. Geotherm. Res.*, doi:10.1016/j.jvolgeores.2017.02.018, 2017.

López, T., Ushakov, S., Izbekov, P., Tassi, F., Cahill, C., Neill, O., and Werner, C.: Constraints on magma processes, subsurface conditions, and total volatile flux at Bezymianny Volcano in 2007–2010 from direct and remote volcanic gas measurements, *J. Volcanol. Geotherm. Res.*, 263, 92–107, doi:10.1016/j.jvolgeores.2012.10.015, 2013.

20 Lübcke, P., Bobrowski, N., Arellano, S., Galle, B., Garzón, G., Vogel, L., and Platt, U.: BrO/SO<sub>2</sub> molar ratios from scanning DOAS measurements in the NOVAC network, *Solid Earth*, 5, 409–424, doi:10.5194/se-5-409-2014, 2014.

Mason, E., Edmonds, M., and Turchyn, A. V.: Remobilization of crustal carbon may dominate volcanic arc emissions, *Science* (New York, N.Y.), 357, 290–294, doi:10.1126/science.aan5049, 2017.

25 Martini, F., Tassi, F., Vaselli, O., Del Potro, R., Martinez, M., van del Laat, R., and Fernandez, E.: Geophysical, geochemical and geodetical signals of reawakening at Turrialba volcano (Costa Rica) after almost 150 years of quiescence, *J. Volcanol. Geotherm. Res.*, 198, 416–432, doi:10.1016/j.jvolgeores.2010.09.021, 2010.

Mather, T. A., Pyle, D. M., Tsanev, V. I., McGonigle, A., Oppenheimer, C., and Allen, A. G.: A reassessment of current volcanic emissions from the Central American arc with specific examples from Nicaragua, *Journal of Volcanology and Geothermal Research*, 149, 297–311, doi:10.1016/j.jvolgeores.2005.07.021, 2006.

30 McBirney, A. R.: The Nicaraguan volcano Masaya and its caldera, *Eos Trans. AGU*, 37(1), 83–96, doi:10.1029/TR037i001p00083, 1956.

McGonigle, A. J. S., Oppenheimer, C., Galle, B., Mather, T. A., and Pyle, D. M.: Walking traverse and scanning DOAS measurements of volcanic gas emission rates, *Geophysical Research Letters*, 29, doi:10.1029/2002GL015827, 2002.

35 McGonigle, A. J. S., Aiuppa, A., Giudice, G., Tamburello, G., Hodson, A. J., and Gurrieri, S.: Unmanned aerial vehicle measurements of volcanic carbon dioxide fluxes, *Geophys. Res. Lett.*, 35, doi:10.1029/2007GL032508, 2008.

Mori, T., Hashimoto, T., Terada, A., Yoshimoto, M., Kazahaya, R., Shinohara, H., and Tanaka, R.: Volcanic plume measurements using a UAV for the 2014 Mt. Ontake eruption, *Earth Planet Sp.*, 68, 1861, doi:10.1186/s40623-016-0418-0, 2016.

40 Oppenheimer, C., Tsanev, V. I., Braban, C. F., Cox, R. A., Adams, J. W., Aiuppa, A., Bobrowski, N., Delmelle, P., Barclay, J., and McGonigle, A. J.: BrO formation in volcanic plumes, *Geochimica et Cosmochimica Acta*, 70, 2935–2941, doi:10.1016/j.gca.2006.04.001, 2006.

Palomaki, R. T., Rose, N. T., van den Bossche, M., Sherman, T. J., and Wekker, S. F. J. de: Wind Estimation in the Lower Atmosphere Using Multirotor Aircraft, *J. Atmos. Oceanic Technol.*, 34, 1183–1191, doi:10.1175/JTECH-D-16-0177.1, 2017.

45 Porter, J. N., Horton, K. A., Mouginis-Mark, P. J., Lienert, B., Sharma, S. K., Lau, E., Sutton, A. J., Elias, T., and Oppenheimer, C.: Sun photometer and lidar measurements of the plume from the Hawaii Kilauea Volcano Pu'u O'o vent: Aerosol flux and SO<sub>2</sub> lifetime, *Geophys. Res. Lett.*, 29, 30-1-30-4, doi:10.1029/2002GL014744, 2002.

Roberts, T. J., Braban, C. F., Martin, R. S., Oppenheimer, C., Adams, J. W., Cox, R. A., Jones, R. L., and Griffiths, P. T.: Modelling reactive halogen formation and ozone depletion in volcanic plumes, *Chem. Geol.*, 263, 151–163, doi:10.1016/j.chemgeo.2008.11.012, 2009.

5 Roberts, T. J., Martin, R. S., and Jourdain, L.: Reactive bromine chemistry in Mount Etna's volcanic plume: The influence of total Br, high-temperature processing, aerosol loading and plume–air mixing, *Atmos. Chem. Phys.*, 14, 11201–11219, doi:10.5194/acp-14-11201-2014, 2014.

10 Roberts, T. J., Saffell, J. R., Oppenheimer, C., & Lurton, T. (2014). Electrochemical sensors applied to pollution monitoring: Measurement error and gas ratio bias at volcano plume case study. *Journal of Volcanology and Geothermal Research*, 281, 85–96. doi:10.1016/j.jvolgeores.2014.02.023, 2014.

15 Roldan, J. J., Joossen, G., Sanz, D., del Cerro, J., and Barrientos, A.: Mini-UAV based sensory system for measuring environmental variables in greenhouses, *Sensors*, 15, 3334–3350, doi:10.3390/s150203334, 2015.

Rüdiger, J., Bobrowski, N., Liotta, M., and Hoffmann, T.: Development and application of a sampling method for the determination of reactive halogen species in volcanic gas emissions, *Anal. Bioanal. Chem.*, 52, 325, doi:10.1007/s00216-017-0525-1, 2017.

Shinohara, H.: A new technique to estimate volcanic gas composition: Plume measurements with a portable multi-sensor system, *J. Volcanol. Geotherm. Res.*, 143, 319–333, doi:10.1016/j.jvolgeores.2004.12.004, 2005.

Symonds, R. B., Rose, W. I., Bluth, G. J. S., and Gerlach, T. M.: Volcanic-gas studies; methods, results, and applications, *Rev. Mineral. Geochem.*, 30, 1–66, 1994.

20 Tamburello, G., McGonigle, A. J., Kantzas, E. P., and Aiuppa, A.: Recent advances in ground-based ultraviolet remote sensing of volcanic SO<sub>2</sub> fluxes, *Annals of Geophysics*, 54, doi:10.4401/ag-5179, 2011.

Theys, N., van Roozendael, M., Dils, B., Hendrick, F., Hao, N., and Mazière, M. de: First satellite detection of volcanic bromine monoxide emission after the Kasatochi eruption, *Geophys. Res. Lett.*, 36, doi:10.1029/2008GL036552, 2009.

Villa, T. F., Gonzalez, F., Miljievic, B., Ristovski, Z. D., and Morawska, L.: An Overview of Small Unmanned Aerial Vehicles for Air Quality Measurements: Present Applications and Future Prospectives, *Sensors*, 16, doi:10.3390/s16071072, 2016.

25 Wittmer, J., Bobrowski, N., Liotta, M., Giuffrida, G., Calabrese, S., and Platt, U.: Active alkaline traps to determine acidic-gas ratios in volcanic plumes: Sampling techniques and analytical methods, *Geochem. Geophys. Geosy.*, 15, 2797–2820, doi:10.1002/2013GC005133, 2014.

York, D., Evensen, N. M., Martínez, M. L., and Basabe Delgado, J. de: Unified equations for the slope, intercept, and standard errors of the best straight line, *Am. J. Phys.*, 72, 367, doi:10.1119/1.1632486, 2004.

30 Zhao, Z. and Wu, Z., *Int. J. Infrared Milli.*, 21, 1607–1615, doi:10.1023/A:1006611609450, 2000.

